Hindawi
Science and Technology of Nuclear Installations
Volume 2021, Article ID 9993614, 10 pages
https://doi.org/10.1155/2021/9993614

Research Article

Study of Clogging Phenomenon for a Conical Hopper: The Influence of Particle Bed Height and Hopper Angle

Muhammad Hammad Khalid and Yixian Zhou

[1]*Beijing Key Laboratory of Passive Safety Technology for Nuclear Energy, North China Electric Power University, Beijing 102206, China*

Correspondence should be addressed to Yixian Zhou; yixian.zhou@ncepu.edu.cn

Received 18 March 2021; Accepted 15 April 2021; Published 26 April 2021

Academic Editor: Iztok Tiselj

The granular flow is one of the principal issues for the design of pebble bed reactors. Particularly, the clogging phenomenon raises an important issue for pebble bed reactors. In this paper, we conduct experiments and discrete particle simulation of two-dimensional discharge granular flow from a conical hopper, to study the effect of the particle bed height h and hopper angle α on the clogging phenomenon. In general, the clogging probability J increases with height h and starts to saturate when h is larger than a critical value. The experimental result trends are supported by discrete simulations. To understand the underlying physical mechanism, we conduct discrete particle simulations for various h values, focusing on the following parameters: the statistical averaging of the volume fraction, velocity, and contact pressure of particles near the aperture during the discharge. We found that, among all relevant variables, the contact pressure of particles is the main cause of the increasement of J when h increases. An exponential law between the pebble bed h and clogging probability J has been established based on these observations and Janssen model. As for hopper angle α, J shows an almost constant behavior for any rise in α followed by a sudden regression at $\alpha = 75^{\circ}$. Surprisingly, the effect of α is most obvious for intermediate values of h, where we observe a sharp increasement of clogging probability. The same trend is observed in the two-dimensional discrete simulation results.

1. Introduction

When a group of discrete particles move downwards inside the hopper, an arch may be formed if the size of the orifice is just a few times larger than the particles, leading to the development of the clogging phenomenon. Clogging occurs just above hopper's aperture, and being a state of static equilibrium, it blocks the overall flow of particles making the system impractical. The phenomenon is not as simple as it appears to be, with its scope quite conceivable ranging from people escaping the room [1, 2] and blockage of industrial granular flow [3] to traffic flow [4]. Clogging also may happen in the core area of pebble bed high-temperature gas-cooled reactor (HTGR). HTGR contains a hopper-shaped core that is being continuously filled with graphite spherical pebbles [5]. This probable formation of arch, shaped in a convex-like structure, is capable enough to jam the system of pebble flow. Once clogging occurs, the refueling stops, initiating stern consequences.

Despite there exist many previous studies, the mechanisms of the clogging process remain unclear. Most previous studies focus on the influence of orifice [6–10]. From the pioneering work of To et al. in 2001 [6], we know that magnitude of clogging probability J changes greatly with the outlet size. Furthermore, the existence of a critical outlet size above which the flow may never get jammed remains debatable [11]. Subsequently, it has been experimentally and numerically shown that some methods can reduce the probability of clogging by, for example, putting an obstacle above the exit [12, 13] and applying a helical texture to the pipes' inner wall [14]. Other variables that have been studied are orifice geometry [15, 16], particle shape [17], particle polydispersity [18], driving force [19, 20], and width of silo [21].

To the best of our knowledge, the role of height of particle bed in the clogging process has not been studied in previous work. The flow pattern of particles before clogging has the resemblance of the flowing particles discharged from a hopper. For the case of flowing discharge flow from a hopper, it has been observed empirically that when the height of particle bed $h > 2.5L$, where L is the hopper width, the flow rate of particles will become independent of the material height h. Such observation accounts for the fact that an hourglass is able to function properly [22]. Probably due to this reason, this parameter has not been studied in previous works. At the exit of the fuel cycle of a typical Chinese 10 MW high-temperature gas-cooled test reactor (HTR-10), the height of the pebble bed does not meet the condition $h > 2.5\,L$, and the exit of the fuel cycle channel resembles a conical hopper with angle below 30°[23, 24]. There exist few works that focus on the influence of hopper angle on granular clogging for high particle bed [6, 25]. The existing work reveals that clogging probability decreases by increasing the hopper angle. The authors noticed a sharp regression in clogging probability for a value of tilt angle α around 75° [6, 25]. The influence of low hopper angle value (lower than 35°) has been ignored. It is reasonable to investigate the probability of the clogging phenomenon under small values of these two parameters. In the present work, we carried out an investigation of the effect of both, the particle bed height h and angle of particle α, on the clogging phenomenon. First, the experimental procedure and discrete simulation are described. The simulation is performed on LMGC90 software, which is based on the NSCD (nonsmooth contact dynamics method) approach. Second, the influence of particle bed height h on the clogging problem has been studied; the experimental result trends are supported by discrete simulations; in order to find the cause for the increment of J when h increases, we conduct discrete particle simulations for various h values, focusing on the statistical averaging of the volume fraction, velocity, and contact pressure of the particles near the aperture during the discharge. An exponential law between the pebble bed h and clogging probability J has been established based on these observations and Janssen model. Finally, the influence of angle of hopper α on the clogging problem has been discussed.

2. Materials and Methods

2.1. Experimental Procedure. The experimental set-up consists of a two-dimensional conical silo with the height of 600 mm, width of 90 mm, and thickness of 3.5 mm. Firm support has been given to the hopper by an aluminum base plate of 4.5 mm in thickness. Front wall comes up with a 4 mm thick sheet, made of perspex to allow visualization. Hopper side walls have been fabricated with aluminum rods of rectangular cross section firmly bolted to the base plate. The base of the hopper is made up of two aluminum rods whose thickness is 3.5 mm just to match the thickness of lateral walls and contains a sleeve inside them so that they can be moved with the help of screws along their length, providing us with the possibility of varying the angle at will. The rectangular outlet is at the center of the bottom of the hopper, with length $D = 18$ mm and thickness W, which is the same as the thickness of the hopper. Note that the thickness of rectangular outlet D is four times larger than the particle diameter d. The apparatus is grounded to prevent the buildup of static electricity.

After filling a monolayer of monodisperse stainless steel disks of 3 mm thickness along with a diameter of $d = 4.5 \pm 0.5$ mm, this weak polydispersity of particles is introduced to avoid the effect of crystallization. With no external drifting force on particles to ensure their discharge course, gravitational force would be the only deciding factor to traverse them out of the hopper. In this paper, the experiment is performed to validate the results obtained by simulation. Following To et al. [6], we have only focused on the clogging probability J for experiments, and other information will be obtained by discrete particle simulations subsequently. The clogging probability J is defined as the ratio of clogging events N_c divided by the number of total trial N_{tt}. N_{tt} is 200. We do not refill the container with particles. The main parameters in this experiment are the particle bed height h, which is the perpendicular distance from the aperture to the level displaced by the particles inside the hopper and the angle of the hopper bottom α (see Figure 1). The dimensions and parameters of test facility are presented in Table 1.

2.2. Simulated System

2.2.1. Discrete Particle Simulation Model and Settings. We performed the simulations by using the open source software LMGC90, which adopts the nonsmooth contact dynamics method (NSCD); this method is based on the concept of rigid spheres and on the implementation of Coulomb's law without regularization. The particles are treated inelastic. Frictional coefficients that have employed to enable contact dissipation are being $\mu_b = 0.4$ and $\mu_w = 0.5$, with the particles and the walls, respectively. A weak polydispersity is set to be $\delta\ d/d = 0.2$ to avoid the crystallization effects. We set the time step to $\delta t = 5 \times 10^{-4}$ s. More simulation details can be found in Zhou et al. [26] and Radjai et al. [27]. We have developed a two-dimensional conical hopper of angle α, orifice size D, and width L (see Figure 2). The orifice is located at the bottom center. We impose $L = 3\ D$ to ensure that silo width does not influence the flow appreciably. Particles with diameter $d = 8$ mm are arranged into granular column by random deposition to diminish the gravitational potential in a closed hopper. First, we have studied the clogging probability J by varying the particle bed height h and angle α. The number of time steps is set long enough to ensure that all particles must get discharged out of the hopper when there would be no occurrence of clogging. 1000 trails have been performed for each case. Second, in order to study the underlying physical mechanism, the statistical averaging of the volume fraction, velocity, and contact pressure of the particles near the aperture during the discharge (before clogging occurs) is measured for various h. The computational domain is periodic in the vertical

Figure 1: A picture of the experimental system when clogging occurs.

Table 1: Test facility dimensions and parameters.

α(°)	h(mm)	D	D	L
0	[50, 100, 120, 150, 200, 350, 500]	4.5 ± 0.5 mm	18	90
15	[50, 100, 120, 150, 200, 350]	4.5 ± 0.5 mm	18	90
30	[50, 100, 120, 150, 200, 350]	4.5 ± 0.5 mm	18	90
45	[50, 100, 120, 150, 200, 350]	4.5 ± 0.5 mm	18	90
75	[50, 100, 120, 150, 200, 350]	4.5 ± 0.5 mm	18	90

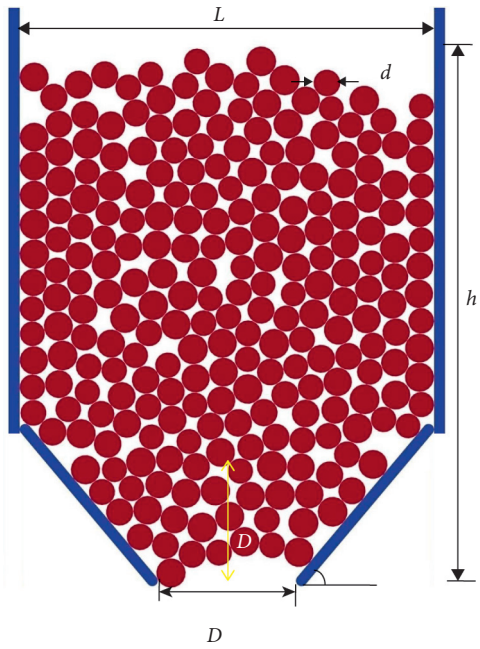

Figure 2: Example of a typical clogging configuration obtained by two-dimensional discrete simulation. Yellow box shows the position where the contact pressure is calculated.

direction to keep constant the number of particles. The vertical boundary of the computational domain has been set to be $10d_m$ above and below the hopper, where d_m is the maximum diameter of the particle. The total number of time step is set to $N_t = 20000$, to ensure the accuracy of the statistical estimation of the average value of volume fraction, velocity, and stress [26]. From the discrete numerical representation of LMGC90, these averages are then computed to examine the processes at the scale of the outlet that could rule the clogging phenomenon at the hopper's scale. The geometry parameters of silo without and with periodic boundary condition are reported in Table 2. Simulation details are reported in Tables 3 and 4 . Specifically, the number of particles N_p and the number of time step N_t for the case without boundary condition are reported in Table 3; the number of particles N_p and the number of time step to calculate the statistical averaging for the case with boundary condition are reported in Table 4.

2.2.2. Postprocessing Method. In this paper, we present an extensive numerical study of the micromechanical properties displayed by granular media flowing through an orifice at the bottom of the hopper. We describe the volume fraction, velocity, and stress of granular media over a confined region near hopper's aperture. Following Zhou et al. [26], we measured the profile of the particle volume fraction $\phi(x)$, the horizontal velocity $u(x)$, and the vertical velocity $v(x)$ at the orifice. The measured region is near the orifice, which is the dashed red box in Figure 3, with a height d. It is the average of the statistics performed over the set of snapshots of a computation during a period of discharge without clogging. For each snapshot, one considers the statistics to be homogeneous over a rectangular domain centered on the measurement location x (see blue box in Figure 3). The width of this rectangle is 0.2 d, which is small with regard to the typical variation of the profiles. The particle volume fraction, $\phi(x)$, is the average over the integration volume (in space and time) of the indicator function, whose value is 1 over the spatial extent of particles and 0 otherwise. According to the ergodicity theorem [28], we can derive the relative accuracy ε of the statistical estimation of the average value as follows [29]:

$$\varepsilon = \frac{\pi d^2}{4\phi N_t \delta t v 0.2\ d}, \tag{1}$$

where v is the average outlet velocity. The velocity profile at the outlet of a particle population is obtained as the ensemble average of the individual particle velocity weighted by their volume intersection with the integration domain. It is therefore the space and time average of the product of the indicator function by the individual velocity divided by ϕ. Since standard deviation of the velocity distribution is small, the convergence of statistics toward the average value is more rapid than for ϕ. The detail of the postprocessing technique can be found in the study by Zhou et al. [26]. By using an averaging process popularized by Goldhirsch et al. [30, 31], we compute the stress tensor from the interparticle forces in the granular medium. The measured region is the

Table 2: Simulations performed without periodic boundary condition to study the clogging probability.

	α (°)	h (mm)	d (mm)	D (d)	L
Without periodic BC	[0, 20, 40, 60, 75]	[75, 150, 300, 450, 600,800,1000]	8	4 d	3 D
With periodic BC	50	[75, 100, 150, 300, 450,600,800,1000,1400,1800]	8	5	3 D

Table 3: Simulations performed in the case without periodic BC for various hopper angles α and particle bed heights h.

(α (°), h (mm))	N_p	N_t
(0, 75)	105	1200
(0, 150)	218	2400
(0, 300)	439	4800
(0, 450)	660	7200
(0, 600)	886	9600
(0, 800)	1176	12800
(0, 1000)	1200	16000
(20, 75)	104	1100
(20, 150)	213	2200
(20, 300)	439	4500
(20, 450)	651	6800
(20, 600)	885	9000
(40, 75)	96	900
(40, 150)	206	1800
(40, 450)	644	5600
(40, 600)	875	7500
(60, 75)	85	600
(60, 150)	191	1300
(60, 300)	412	2600
(60, 450)	631	3900
(60, 600)	856	5200
(75, 75)	59	400
(75, 150)	160	800
(75, 300)	377	1600
(75, 450)	603	2400
(75, 600)	827	3200

N_p: the number of particles; N_t: the number of time steps.

Table 4: Simulations performed in the case with periodic BC for a fixed hopper angle $\alpha = 50^\circ$ and various particle bed heights h.

h (mm)	N_p	N_t^a
75	107	18972
100	161	18428
150	247	17904
300	527	17984
450	800	10080
600	1084	10046
800	1458	5006
1000	1841	4830
1400	2377	8124
1800	3352	3278

N_p: the number of particles; N_t^a: the number of time step to calculate the statistical averaging.

yellow box in Figure 2. Let us consider at time t a set of N particles indexed by α, having the mass m_i, whose centers of mass are x^α and which move with a speed u^α. The macroscopic stress field σ_{ij} can be decomposed into a contact stress field related with particle-particle interactions and a kinetic stress field which is induced by the fluctuating

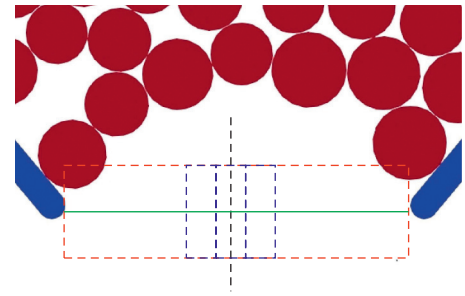

Figure 3: Snapshot of a typical clogging arch. Red (green) box (line) shows the position where the volume fraction and velocity are determined. Blue box is centered at a position x, and it shows where we determine the volume fraction and velocity at the position x.

motion of grains, which carry their momentum from one place to another. By choosing a common step function, the definition of the stress tensor is equivalent to

$$\sigma_{ij} = -\frac{1}{V}\sum_{\alpha\in V} m_i u_i^{'\alpha} u_j^{'\alpha} - \frac{1}{V}\sum_{c\in V} f_i^c b_j^c, \tag{2}$$

where $u^{'\alpha}(x,t)$ is the fluctuating velocity of particle α. The second sum is performed over the contacts c inside the volume V. Here, f^c is the interaction force modulus between the two particles in contact in c. The vector b^c is called the branch vector and is equal to the vector $x^{\alpha\beta}$ connecting the centers of two particles α and β forming the contact c if α and β belong to the volume but is equal to the portion of this vector included in V if one particle is outside the volume V. The trace of the stress tensor is defined as the contact pressure. Figure 4 shows the contact pressure of a typical case with $h = 600$ mm, which is compatible with the contact pressure field obtained in Rubio-Largo's work [32].

3. Results and Discussion

3.1. Influence of Particle Bed Height. We studied the effects of height h on clogging probability J. Figure 5 plots J with respect to h under various hopper angles α, where Figure 5(a) and Figure 5(b) show the experiment results and simulation results, respectively.

From Figure 5(a), we can see that the clogging probability J increases with height h and starts to saturate when h is larger than 0.18m. With $\alpha = 75^\circ$, J decreases sharply for any particle bed height h. For smaller and greater heights h, apart from that clogging decreases sharply at $\alpha = 75^\circ$, no appreciable difference in clogging can be seen by transforming the inclination of hopper walls. The influence of hopper angle will be further discussed in the next section. The same trend has also been observed in simulation results (see Figure 5(b)); the clogging probability J increases with height h and starts to saturate when h is larger than 3.75L.

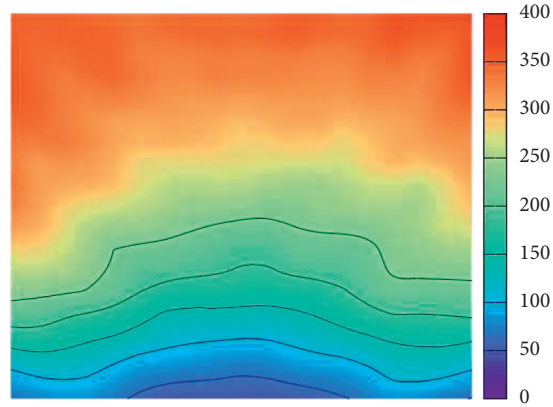

Figure 4: The contact pressure $\mathrm{tr}[\sigma_{ij}]$ (Pa) near the orifice (a zone at the yellow box shown in Figure 2) for a typical case with $h = 600$ mm.

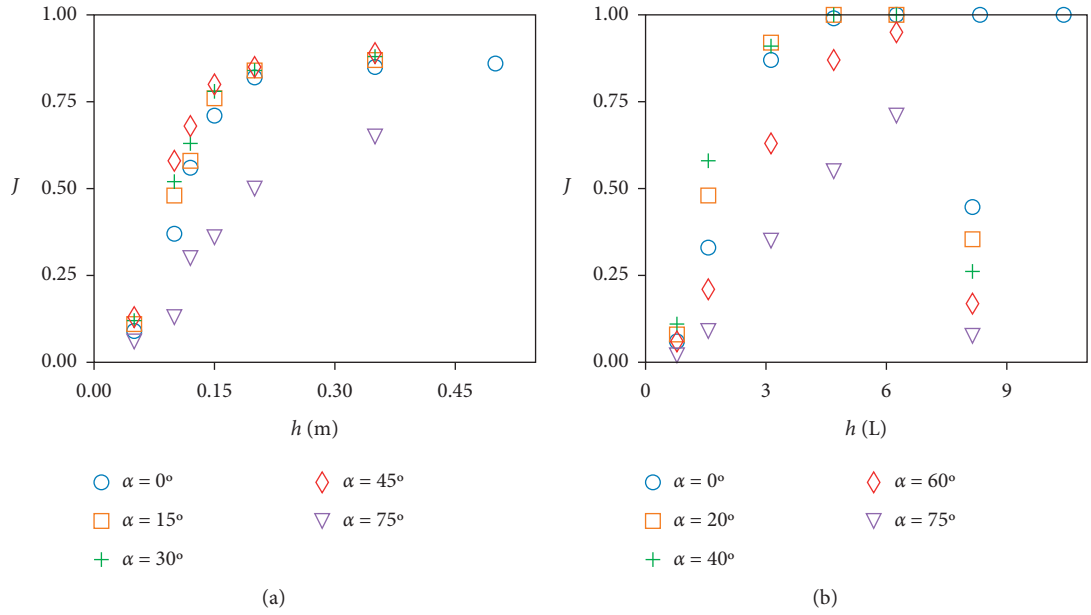

Figure 5: Results of clogging probability J versus pebble bed height h for various tilt angles α obtained by (a) experiment and (b) simulation.

In order to explore the underlying physical mechanism of the influence of particle bed h, we have performed the discrete element simulation with periodic condition. The parameters for the simulation are also found in Tables 1 and 3. First, following Zhou et al. [26], we investigated the volume fraction and velocity profiles near the outlet. Figure 6(a) shows the measured particle volume fraction at the outlet, as a function of the horizontal position x normalized by the diameter of the outlet D for various heights h. We can observe that as the height h increases, the data points tend to overlap with each other. Average values of volume fraction $\overline{\phi}$ are plotted versus the particle bed height h normalized by the hopper width L in Figure 6(b). With different h/L values, the average values of volume fraction $\overline{\phi}$ remain constant. The error bars represent the relative accuracy ε given by equation (1) which is around 0.8%. Regardless of any effect induced by pebble bed height h, we observed a relatively constant behavior in volume fraction with a minute surge at elevated h values. The difference between the maximum and minimum values is 2.7 percent of the minimum value. In the case of flowing particles without clogging, the variation of volume fraction at the center of the outlet depends on the outlet size and on the particle diameter, exhibiting a dilatancy for small aperture in order to maintain the flow of the material [26, 33]. From the results displayed in Figure 6, it can be concluded that the change of height of particles bed does not influence the dilatancy at the outlet. Namely, the volume fraction does not contribute to the variation of clogging probability J when h varies.

In the same way, the profiles of the horizontal component of velocity, $u(x)$, and the profiles of the vertical component of the velocity, $v(x)$, for various column heights are plotted, respectively, in Figures 7(a) and 7(b). The horizontal velocity depends linearly on x, and it increases.

As we move away on either side from the central axis of the hopper at the outlet, these profiles show that the particle flow has a horizontal component towards the center. These

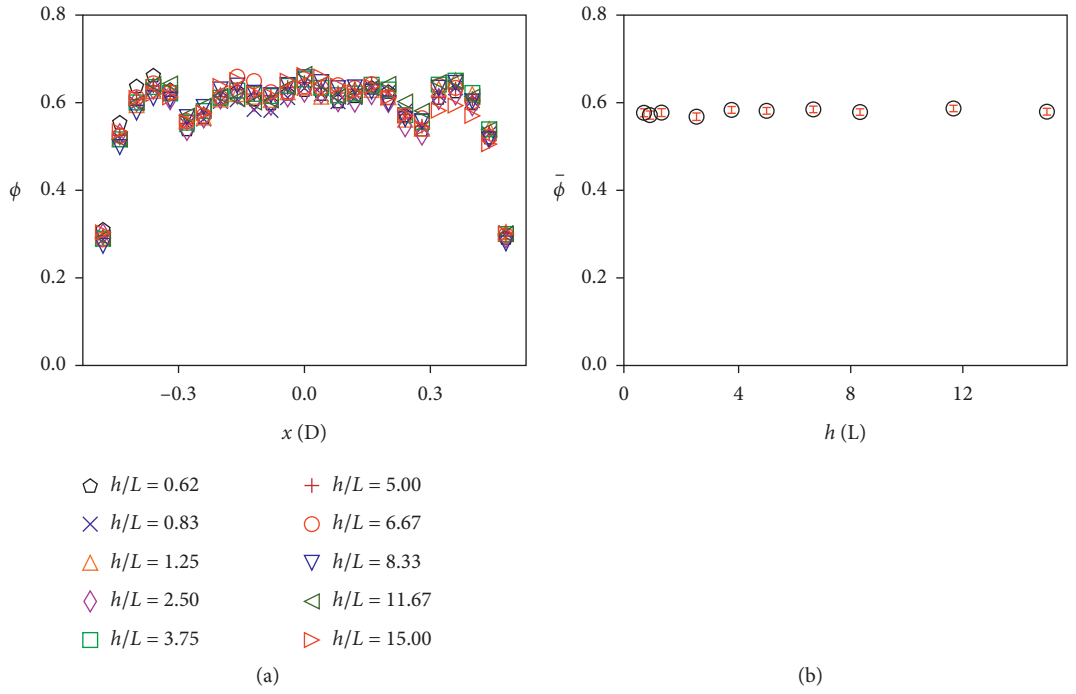

Figure 6: Results of volume fraction for different pebble bed heights h. (a) Horizontal profiles of the volume fraction versus the position x normalized by the orifice size D for various particle bed heights. (b) Average values of volume fraction $\overline{\phi}$ versus the particle bed height h normalized by the hopper width L.

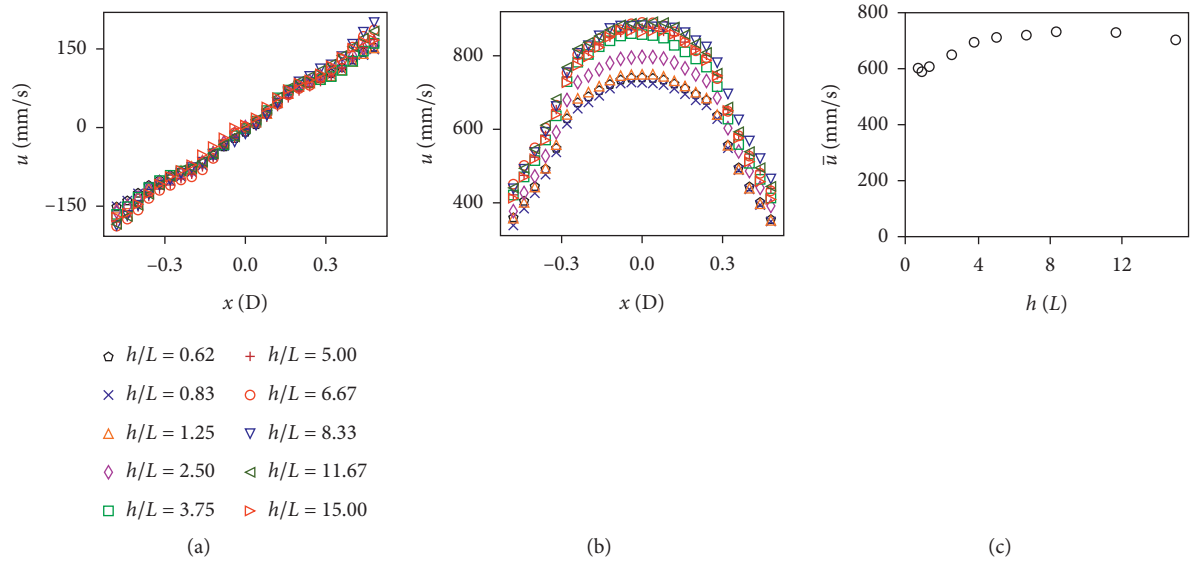

Figure 7: Results of velocity for different pebble bed heights h. (a) Horizontal profiles of the horizontal velocity u. (b) Horizontal profiles of the vertical velocity v. (c) Mean vertical velocity $\overline{v}$ versus the height of the particle bed h normalized by hopper width L.

values of horizontal velocity are independent of the pebble bed height h. Figure 7(b) reveals that the vertical velocity profiles are quasiparabolic and depend on the particle bed height. The evolution of the average value of vertical velocity $\overline{v}$ versus the particle bed height normalized by hopper width h/L is plotted in Figure 7(c). We can observe that, as the pebble bed heights increase, the vertical velocities would also rise. It has been observed experimentally that when the driving force increases, the clogging probability decreases. Arevalo et al. [19] found that the physical magnitude behind clogging reduction by increasing gravity or particle density is the averaged kinetic energy per particle. Assuming that the kinetic energy of the particles is related to the total kinetic energy, the higher the kinetic energy, the longer it takes to

the system to stabilize, and during this time is when the particles can keep flowing, it seems reasonable that increasing the kinetic energy decreases the clogging probability. In our case, when h increases, the kinetic energy increases but the clogging probability increases; this suggests that the physical magnitude behind this clogging increment by increasing the particle bed height h is not the kinetic energy.

Next, we investigated the results of contact pressure $\mathrm{tr}[\sigma_{ij}]$ at a region close to the outlet (see the yellow box in Figure 2); $\mathrm{tr}[\sigma_{ij}]$ at the vertical central line of the region mentioned above is plotted against vertical position y normalized by the diameter of the outlet D for various heights h (see Figure 8(a)). We can observe that the contact pressure increases with the vertical position and saturates at a certain position. The contact pressure at the position $y = D$ is plotted against h/L in Figure 8(b); one can see that it depends strongly on the particle bed height and starts to saturate when h/L is larger than 5. We can conclude that, among all relevant variables, the contact pressure of particles is the main cause of the increasement of J when h increases.

In 1895, Janssen proposed a model in which they measured the pressure at the bottom of a silo filled with corn [34]. They noticed that as long as the corn keeps being filled, pressure saturates, which is different from the case of liquids. In light of Janssen's model, we will establish a naive relationship between the clogging probability J and particle bed height h. First of all, we will study the contact pressure on the upper edge of the square shown as the yellow box in Figure 2 on the position $y = D$. According to Janssen's model, the vertical stress at $y = D$ is given by

$$\sigma_{yy} = A_1\left(1 - e^{-(h-D)/A_2}\right), \tag{3}$$

where A_1 and A_2 are constants which depend on the geometry and material of particles and hopper. According to Janssen's assumption, the horizontal normal stress is proportional to the vertical normal stress, and the contact pressure can be written as follows:

$$\mathrm{tr}\left[\sigma_{ij}\right] = B_1\left(1 - e^{-B_2 h + B_3}\right), \tag{4}$$

where B_1, B_2, and B_3 are fitting parameters. We adjusted the simulation data of the contact pressure near the orifice by equation (4) by using the least-squares method (see black dotted line in Figure 8(b), where the contact pressure at location $y = D$ is plotted versus the particle bed height). The agreement is found to be fairly good, which validates equation (4).

Next, we hypothesize that the clogging probability J depends linearly with the contact pressure of the particles when the particles are static before opening the orifice. We can deduce that the relationship between clogging probability J and pebble bed height h is written as follows:

$$J = J_{\mathrm{inf}}\left(1 - e^{-C_1 h + C_2}\right). \tag{5}$$

J_{inf} represents the clogging probability when h tends towards infinity. This value depends on other parameters (like orifice size) of the system, and there exist some empirical models of this value [11]. C_1 and C_2 are the fitting parameters. We plotted J versus $h\,(m)$ with the flat-bottom hopper ($\alpha = 0^\circ$) for experiment and simulation in Figure 9(a) and 9(b), respectively. We adjusted the experimental and simulation data by equation (5) by using the least-squares method (see black dashed line); the fitting parameters are $C_1 = 13.92$ and $C_2 = 0.62$ for experiment and $C_1 = 7.25$ and $C_2 = 0.53$ for simulation. We can see that in two cases, C_1 is an order of magnitude larger than C_2. When h tends to infinity, we obtain clogging probability $J_{\mathrm{inf}} = 0.86$ in the experiments and $J_{\mathrm{inf}} = 1$ in simulation. We can see that the particles are more likely to jam in simulation; this is perhaps due to the reason that the experiment is quasi-2D which differs from a 2D case.

3.2. Influence of Hopper Angle. As we can observe from Figure 5 that clogging probability depends on hopper angle, here we replot Figure 5 to better illustrate the influence of hopper angle. Figure 10 plots J with respect to α under various particle beds h, where Figures 10(a) and 10(b) show the experiment results and simulation results, respectively. From Figure 10(a), we can see that J shows an almost constant behavior for any rise in α followed by a sudden regression for $\alpha = 75^\circ$. However, for intermediate values of h, we have noticed a sharp increasement in clogging till $\alpha = 75^\circ$. This trend has been perceived mostly at $h = 0.1$ m. At a particle bed height $h = 0.1$ m, J has proved to be affected by α at its maximum. A clogging maximum has been attained at $\alpha = 45^\circ$ that has not been affected by particle heights.

The same trend has been observed for simulation results in Figure 10(b). J increases with α for intermediate values of h/L when a maximum value has been attained at $\alpha = 40^\circ$ and starts to decrease at $\alpha = 60^\circ$. It has been revealed that a convincing correlation exists between the hopper angle and the nature of flow of particles. For lower angles, the nature of flow is of funnel type, at which particles along the central axis of the hopper move faster than the ones closer to the walls since frictional effects dominate so that only a portion of particles can move while others form a stagnant zone [35]. Rose and Tanaka [36] found that due to the presence of a stagnant zone near the opening, the flow rate in a hopper does not depend on α if α is less than a critical value α_r related to the angle of stagnant zone. Before clogging occurs, the flow of particles in our clogging experiment has the resemblance of the discharge of flow from hopper. It is possible that in our experiment, α_r is between 45° and 70° so that the clogging probability is almost constant for $\alpha \leq 75^\circ$. For hopper angle $\alpha = 75^\circ$, the clogging probability J decreases sharply; this is reasonable since at the extreme value when $\alpha = 90^\circ$, clogging should not occur when $D > d$. However, the surge of clogging probability J for intermediate values h is somewhat unexpected. It is probably due to the augmentation of contact pressure. Currently simulations are being carried out for further study of this effect.

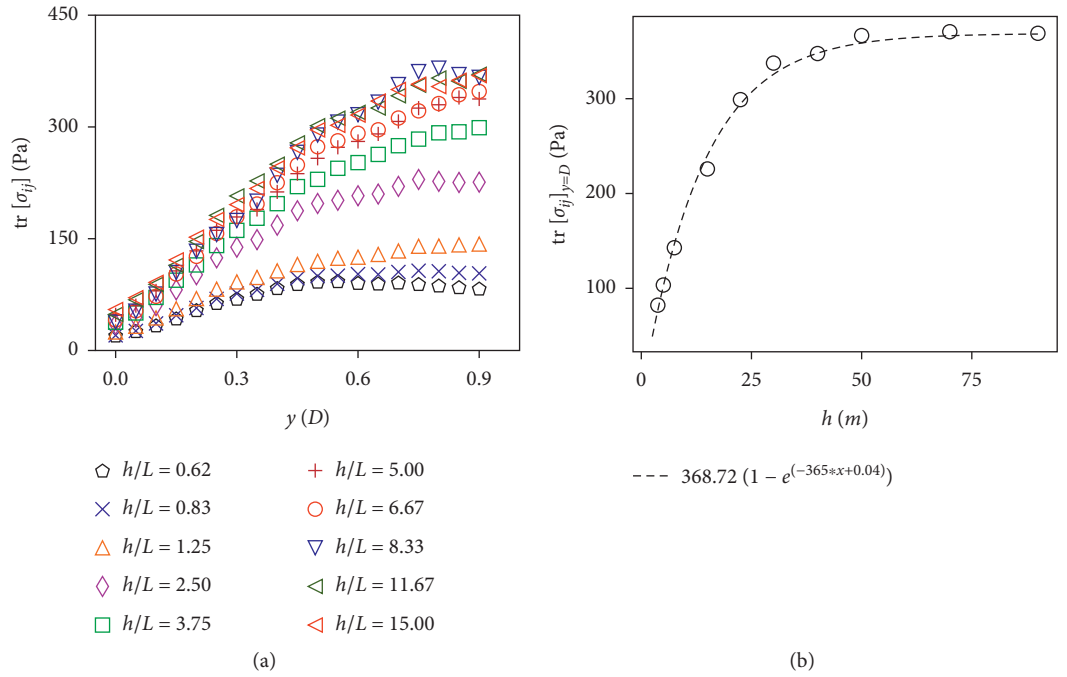

Figure 8: Results of contact pressure $\mathrm{tr}[\sigma_{ij}]$ near the orifice. (a) Contact pressure $\mathrm{tr}[\sigma_{ij}]$ at the vertical central line of the yellow box shown in Figure 2 against vertical position y normalized by the diameter of the outlet D for various heights h. (b) The contact pressure on the upper edge of the square shown as the yellow box in Figure 2 $\mathrm{tr}[\sigma_{ij}]|_{y=D}$ versus the particle bed height h.

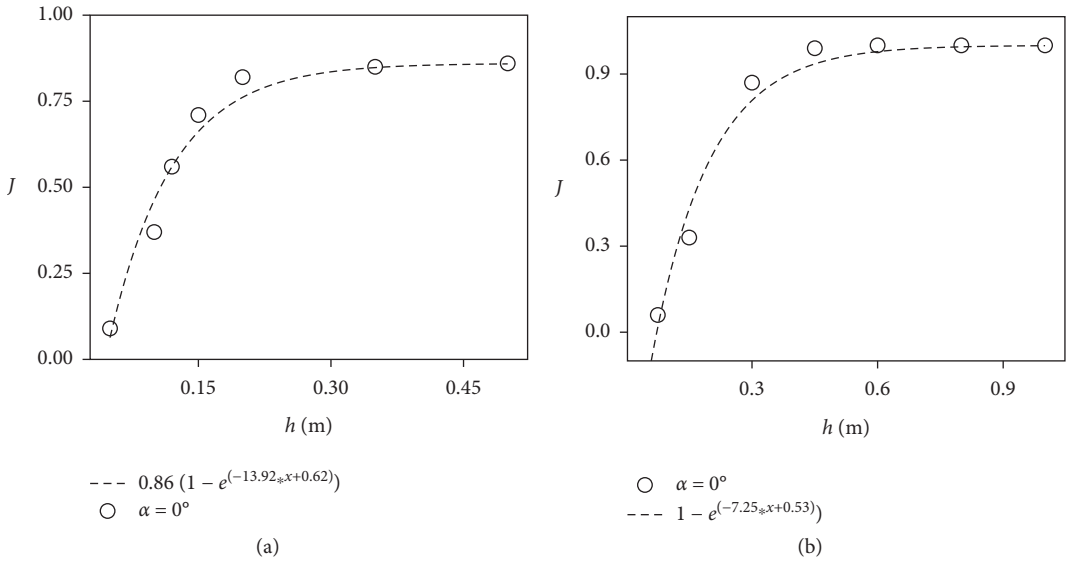

Figure 9: Results of clogging probability J versus pebble bed height h for flat-bottom hopper ($\alpha = 0^{\circ}$) obtained by (a) experiment and (b) simulation. The dashed lines represent equation (5) with $J_{\mathrm{inf}} = 0.86$, $C_1 = 13.92$, and $C_2 = 0.62$ in (a) (respectively, $J_{\mathrm{inf}} = 1$, $C_1 = 7.25$, and $C_2 = 0.53$ in (b)).

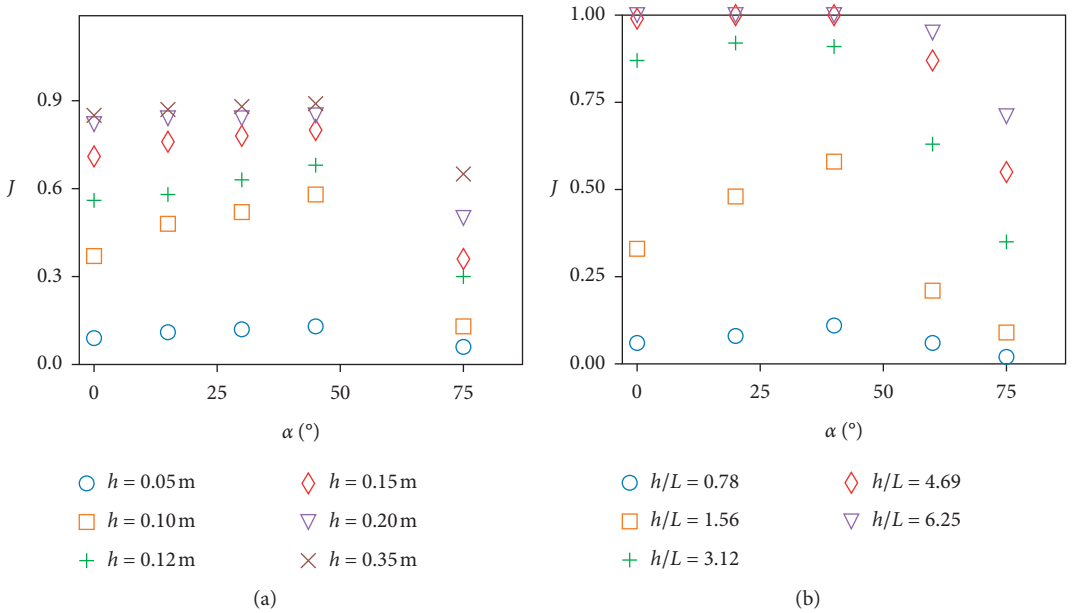

FIGURE 10: Results of clogging probability J versus hopper angle α for various pebble bed heights h obtained by (a) experiment and (b) simulation.

4. Conclusions

In this paper, discrete numerical simulations and experiments are conducted to study the influence of container's geometry on the clogging phenomenon. The height of the pebble bed h and the angle of the conical hopper α are our varied parameters. The volume fraction, the velocity, and the contact pressure profiles through the aperture were measured to study the underlying physical mechanism. According to the results, some conclusions were drawn as follows:

(1) The clogging probability J increases with height h and starts to saturate when h is larger than a certain value, suggesting that flow becomes more susceptible to clog if we increase h. This behavior is consistent for every hopper angle.

(2) Based on the results of volume fraction near the orifice, we observe a weak variation of volume fraction ϕ when varying particle bed height h, suggesting that the change of height of particles bed does not influence the dilatancy at the outlet. We can conclude that the volume fraction at the outlet does not contribute to the augmentation of clogging probability J when h increases.

(3) The results suggest that the physical magnitude behind this clogging increment by increasing the particle bed height h is not the kinetic energy.

(4) The contact pressure near the orifice depends strongly on the particle bed height and starts to saturate when h is larger than a certain value. It thus has an imperative effect on the probability of clogging. An exponential law between the pebble bed h and clogging probability J has been established based on these observations and Janssen model.

Data Availability

The data used to support the findings of this study are available from the corresponding authors upon request.

Conflicts of Interest

The authors declare that they have no conflicts of interest.

Acknowledgments

This project was supported by the National Natural Science Foundation of China (Grant no. 11802094).

References

[1] D. Helbing and P. Molnár, "Social force model for pedestrian dynamics," *Physical Review E*, vol. 51, no. 5, pp. 4282–4286, 1995.

[2] D. Helbing, I. Farkas, and T. Vicsek, "Simulating dynamical features of escape panic," *Nature*, vol. 407, no. 6803, pp. 487–490, 2000.

[3] J. Johanson and W. Kleysteuber, "Flow corrective inserts in bins," *Chemical Engineering Progress*, vol. 62, pp. 79–83, 1966.

[4] D. Helbing, A. Johansson, J. Mathiesen et al., "Analytical approach to continuous and intermittent bottleneck flows," *Physical Review Letters*, vol. 97, no. 16, Article ID 168001, 2006.

[5] A. C. Kadac and M. Z. Bazant, "Pebble flow experiments for pebble bed reactors," in *Proceedings of the 2nd International Topical Meeting on High Temperature Reactor Technology*, Beijing, China, September 2004.

[6] K. To, P.-Y. Lai, and H. K. Pak, "Jamming of granular flow in a two-dimensional hopper," *Physical Review Letters*, vol. 86, no. 1, pp. 71–74, 2001.

[7] I. Zuriguel, A. Garcimartín, D. Maza et al., "Jamming during the discharge of granular matter from a silo," *Physical Review E*, vol. 71, no. 5, Article ID 051303, 2005.

[8] K. To, "Jamming transition in two-dimensional hoppers and silos," *Physical Review E*, vol. 71, no. 6, Article ID 060301, 2005.

[9] A. Janda, I. Zuriguel, A. Garcimartín et al., "Jamming and critical outlet size in the discharge of a two-dimensional silo," *Europhysics Letters*, vol. 84, no. 4, Article ID 44002, 2008.

[10] C. C. Thomas and D. J. Durian, "Fraction of clogging configurations sampled by granular hopper flow," *Physical Review Letters*, vol. 114, no. 17, Article ID 178001, 2015.

[11] D. Gella, I. Zuriguel, and D. Maza, "Decoupling geometrical and kinematic contributions to the silo clogging process," *Physical Review Letters*, vol. 121, no. 13, Article ID 138001, 2018.

[12] I. Zuriguel, A. Janda, A. Garcimartín et al., "Silo clogging reduction by the presence of an obstacle," *Physical Review Letters*, vol. 107, no. 27, Article ID 278001, 2011.

[13] K. Endo, K. A. Reddy, and H. Katsuragi, "Obstacle-shape effect in a two-dimensional granular silo flow field," *Physical Review Fluids*, vol. 2, no. 9, Article ID 094302, 2017.

[14] F. Verbücheln, E. J. R. Parteli, T. Pöschel et al., "Helical inner-wall texture prevents jamming in granular pipe flows," *Soft Matter*, vol. 11, no. 21, pp. 4295–4305, 2015.

[15] C. C. Thomas and D. J. Durian, "Geometry dependence of the clogging transition in tilted hoppers," *Physical Review E*, vol. 87, no. 5, Article ID 052201, 2013.

[16] S. Saraf and S. V. Franklin, "Power-law flow statistics in anisometric (wedge) hoppers," *Physical Review E*, vol. 83, no. 3, Article ID 030301, 2011.

[17] A. Ashour, S. Wegner, T. Trittel, T. Börzsönyi, and R. Stannarius, "Outflow and clogging of shape-anisotropic grains in hoppers with small apertures," *Soft Matter*, vol. 13, no. 2, pp. 402–414, 2017.

[18] L. Pournin, M. Ramaioli, P. Folly et al., "About the influence of friction and polydispersity on the jamming behavior of bead assemblies," *The European Physical Journal E*, vol. 23, p. 229, 2007.

[19] R. Arévalo, I. Zuriguel, D. Maza et al., "Role of driving force on the clogging of inert particles in a bottleneck," *Physical Review E*, vol. 89, no. 4, Article ID 042205, 2014.

[20] R. Arévalo and I. Zuriguel, "Clogging of granular materials in silos: effect of gravity and outlet size," *Soft Matter*, vol. 12, no. 1, pp. 123–130, 2016.

[21] D. Gella, D. Maza, I. Zuriguel et al., "Linking bottleneck clogging with flow kinematics in granular materials: the role of silo width," *Physical Review Fluids*, vol. 2, no. 8, Article ID 084304, 2017.

[22] D. Hirshfeld and D. Rapaport, "Granular flow from a silo: discrete-particle simulations in three dimensions," *The European Physical Journal E*, vol. 4, p. 193, 2001.

[23] Z. Zhang, Z. Wu, D. Wang et al., "Current status and technical description of Chinese 2×250 MW th HTR-PM demonstration plant," *Nuclear Engineering and Design*, vol. 239, no. 7, pp. 1212–1219, 2009.

[24] A. G. Rodríguez, L. Y. R. Mazaira, C. R. G. Hernández et al., "An integral 3D full-scale steady-state thermohydraulic calculation of the high temperature pebble bed gas-cooled reactor HTR-10," *Nuclear Engineering and Design*, vol. 373, Article ID 111011, 2021.

[25] D. López-Rodríguez, D. Gella, K. To et al., "Effect of hopper angle on granular clogging," *Physical Review E*, vol. 99, no. 3, Article ID 032901, 2019.

[26] Y. Zhou, P. Ruyer, and P. Aussillous, "Discharge flow of a bidisperse granular media from a silo: discrete particle simulations," *Physical Review E*, vol. 92, no. 6, Article ID 062204, 2015.

[27] Radjai and F. Dubois, *Discrete-element Modeling of Granular Materials*, Wiley-Iste, London, UK, 2011.

[28] M. Einsiedler and T. Ward, *Ergodic Theory: with a View Towards Number Theory*, Springer-Verlag, London, UK, 2011.

[29] Y. Zhou, "Universite d'Aix-Marseille," 2016.

[30] B. J. Glasser and I. Goldhirsch, "Scale dependence, correlations, and fluctuations of stresses in rapid granular flows," *Physics of Fluids*, vol. 13, no. 2, pp. 407–420, 2001.

[31] C. Goldenberg and I. Goldhirsch, "Force chains, microelasticity, and macroelasticity," *Physical Review Letters*, vol. 89, no. 8, Article ID 084302, 2002.

[32] S. M. Rubio-Largo, A. Janda, D. Maza et al., "Disentangling the free-fall arch paradox in silo discharge," *Physical Review Letters*, vol. 114, Article ID 238002, 2015.

[33] A. Janda, I. Zuriguel, and D. Maza, "Flow rate of particles through apertures obtained from self-similar density and velocity profiles," *Physical Review Letters*, vol. 108, no. 24, Article ID 248001, 2012.

[34] B. P. Tighe and M. Sperl, "Pressure and motion of dry sand: translation of Hagen's paper from 1852," *Granular Matter*, vol. 9, no. 3-4, pp. 141–144, 2007.

[35] Q. J. Zheng and A. B. Yu, "Finite element investigation of the flow and stress patterns in conical hopper during discharge," *Chemical Engineering Science*, vol. 129, pp. 49–57, 2015.

[36] H. E. Rose and T. Tanaka, "Disentangling the free-fall arch paradox in silo discharge," *Engineer (London)*, vol. 208, p. 465, 1959.